

# Andrographolide enhanced radiosensitivity by downregulating glycolysis via the inhibition of the PI3K-Akt-mTOR signaling pathway in HCT116 colorectal cancer cells

Journal of International Medical Research  
48(8) 1–17

© The Author(s) 2020

Article reuse guidelines:

[sagepub.com/journals-permissions](https://sagepub.com/journals-permissions)

DOI: [10.1177/0300060520946169](https://doi.org/10.1177/0300060520946169)

[journals.sagepub.com/home/imr](https://journals.sagepub.com/home/imr)



Xiaofei Li<sup>1,\*</sup>, Ruifang Tian<sup>1,\*</sup> , Lan Liu<sup>1</sup>,  
Lihui Wang<sup>1</sup>, Dong He<sup>2</sup>, Ke Cao<sup>1</sup>, John K. Ma<sup>3</sup>  
and Chenghui Huang<sup>1</sup> 

## Abstract

**Objective:** Radiotherapy plays an important role in the treatment of colorectal cancer (CRC). However, some patients benefit minimally from radiotherapy because of radioresistance. This study investigated the effects of andrographolide on radiosensitivity in HCT116 CRC cells and examined its mechanism of action.

**Methods:** Cell survival, proliferation, apoptosis, and migration were evaluated using MTT, colony formation, flow cytometry, and Transwell cell invasion assays, respectively. Glycolysis-related indicators were measured to examine cell glycolytic activity. The expression of related proteins was detected by western blotting.

**Results:** After andrographolide treatment, the expression of phosphoinositide 3-kinase (PI3K)-Akt-mammalian target of rapamycin (mTOR) signaling pathway-related proteins, glycolytic activity, and cell survival and invasion rates were decreased in HCT116 cells. Andrographolide plus irradiation increased apoptosis and decreased survival, invasion, and colony formation compared with the effects of irradiation alone.

<sup>1</sup>Department of Oncology, The Third Xiangya Hospital, Central South University, Changsha, Hunan, China

<sup>2</sup>Department of Respiratory, The Second People's Hospital of Hunan Province, Changsha, Hunan, China

<sup>3</sup>Cotton O'Neil Cancer Center, Stormont Vail Hospital, Topeka, KS, USA

\*These authors contributed equally to this work.

## Corresponding author:

Chenghui Huang, The Third Xiangya Hospital, Central South University, Tongzipo Road 138, Changsha 410013, Hunan, China.

Email: [86801158@qq.com](mailto:86801158@qq.com)



**Conclusion:** Andrographolide enhanced radiosensitivity by downregulating glycolysis via inhibition of the PI3K-Akt-mTOR signaling pathway in HCT116 cells.

### Keywords

Colorectal cancer, andrographolide, glycolysis, radiosensitivity, PI3K-Akt-mTOR pathway, apoptosis, migration, invasion

Date received: 16 March 2020; accepted: 9 July 2020

### Introduction

Colorectal cancer (CRC) is a global public health problem. According to the American Cancer Society epidemiological statistics in 2019, CRC was the third most common cause of cancer-related morbidity and mortality worldwide.<sup>1</sup> Currently, surgery remains the standard of care for CRC, and radiotherapy plays an important role in its comprehensive treatment. However, some patients with CRC who receive radiotherapy have a poor prognosis because of radioresistance.<sup>2</sup> Increasing the radiation dose aggravates damage in healthy tissues and organs around the tumor and seriously affects patients' quality of life.<sup>3</sup> Therefore, the identification of novel radiosensitizers with low toxicity and high efficiency are current challenges in radiation oncology.

*Andrographis paniculata* is a species of Andrographideae. Its main active ingredients are diterpene lactone compounds and andrographolide, which have been demonstrated to possess anti-cancer, anti-inflammatory, anti-viral, and immunomodulatory properties.<sup>4</sup>

The anti-cancer mechanisms of andrographolide include the induction of apoptosis and cell cycle arrest and inhibition of tumor angiogenesis.<sup>5</sup> Andrographolide has been revealed to enhance the radiosensitivity of tumors through a variety of mechanisms. The agent can increase miR-218 expression in oral squamous cell carcinoma, increase the protein levels of cleaved

caspase 3/Bax, and decrease the expression of Bcl-2/NF- $\kappa$ B in esophageal ECA109 cells.<sup>6,7</sup> However, studies focusing on whether andrographolide enhances the radiosensitivity of CRC cells have not been reported.

Andrographolide can inhibit the phosphatidylinositol-4,5-bisphosphate 3-kinase catalytic subunit alpha-Akt1-mammalian target of rapamycin (mTOR)-ribosomal protein S6 kinase B1 pathway, triggering mitochondrial autophagy, the reversal of mitochondrial membrane potential disintegration, and inactivation of the NLR family pyrin domain-containing 3 (NLRP3) inflammasome, thereby preventing colitis-associated cancer.<sup>8</sup> The phosphoinositide 3-kinase (PI3K)-Akt-mTOR signaling pathway also plays an important part in regulating glycolysis.<sup>9</sup> While exploring its mechanisms of action in treating diabetes, it was found that andrographolide affects the activity and expression of glycolysis-related proteins in liver cells, such as glucose transporter 4 (GLUT4), hexokinase (HK), and glucose-6 phosphatase. Nevertheless, the role of andrographolide in glucose metabolism in tumor cells remains unclear.<sup>10,11</sup>

Reprogramming of energy metabolism, especially cellular glucose metabolism, is an important characteristic of malignant tumors. Even in the presence of adequate oxygen, tumor cells tend to initiate relatively low-efficiency glycolysis to metabolize glucose. This phenomenon is known as the

Warburg effect.<sup>12</sup> Many studies illustrated that radioresistance is closely related to glycolysis in tumor cells.<sup>13–15</sup> We found that phosphofructokinase-1 (PFK1) depletion enhanced radiosensitivity in HT29 and HCT116 cells. Girdin is a protein that can regulate glycolysis in hepatocellular carcinoma cells through the PI3K-Akt-HIF-1 $\alpha$  signaling pathway, thereby decreasing the sensitivity of HepG2 and Huh-7 cells to irradiation *in vitro* and *in vivo*.<sup>16</sup> However, the effect of andrographolide on glycolysis and its correlation with radiosensitivity in CRC cells has rarely been studied.

In this study, we investigated the effects of andrographolide on glycolysis and radiosensitivity, as well as the potential mechanisms through modulation of the PI3K-Akt-mTOR signaling pathway in HCT116 cells. We first sought to identify the appropriate andrographolide concentration. We then explored the mechanism by which andrographolide regulated proliferation and glycolysis and enhanced radiosensitivity in HCT116 cells by targeting the PI3K-Akt-mTOR signaling pathway. The results of this study may provide a scientific basis by which andrographolide enhances radiosensitivity in HCT116 cells.

## Materials and methods

### Key reagents

Andrographolide was purchased from Shanghai Yuanye Bio-Technology (Shanghai, China) and dissolved in DMSO (Sigma-Aldrich Chemical Co., St. Louis, MO, USA) to obtain a stock solution of 100 mM. Insulin-like growth factor 1 (IGF-1, a PI3K activator) was purchased from Puxin Bio (Shanghai, China), and LY294002 (a PI3K inhibitor) was purchased from AbMole China (Shanghai, China).

### Cell culture

Human HCT116 cells were purchased from the American Type Culture Collection (Manassas, VA, USA) and cultured in Dulbecco's modified Eagle's medium (DMEM, Gibco, Thermo Fisher Scientific, Waltham, MA, USA) containing 10% fetal bovine serum at 37°C in a 5% CO<sub>2</sub> incubator. The study was approved by the Medical Ethics Committee of the Third Xiangya Hospital of Central South University on 4 April 2019.

### X-ray irradiation

The Varian TrueBeam linear accelerator (Varian, Palo Alto, CA, USA) was used to irradiate cells at a fixed dose rate of 2 Gy/min. Cells were irradiated with various doses according to set parameters. The graded doses of X-rays used to irradiate cells were 0, 2, 4, 6, and 8 Gy.

### MTT assay

HCT116 cells were seeded into a 96-well plate at a density of  $1 \times 10^4$  cells/well in 100  $\mu$ L of DMEM. Subsequently, the cells were incubated for 48 hours at 37°C in an atmosphere of 5% CO<sub>2</sub> and 100% humidity with graded doses of andrographolide. Fifty microliters of MTT reagent (5 mg/mL, Applygen, Beijing, China) were added to each well, and the plate was incubated for another 4 hours at 37°C. The MTT solution was removed, and 150  $\mu$ L of DMSO were added to each well to dissolve the purple formazan crystals. The optical density of each well was measured using a Microplate Reader (Bio-Rad, CA, USA) at a wavelength of 570 nm. Cell proliferation was expressed as a percentage of the control.

### Glycolysis assay

Glycolytic activity was measured using glucose assay, lactic acid assay, ATP assay,

and PFK1 activity kits, all of which were purchased from Bioengineering Institute (Nanjing, China). The kits were used to measure glucose consumption, lactic acid production, ATP production, and PFK1 activity, respectively, in HCT116 cells following the manufacturer's instructions.

### **Apoptosis assay**

Cell apoptosis was detected *in vitro* via flow cytometry after staining cells with annexin V-fluorescein isothiocyanate-propidium iodide using an apoptosis detection kit (Sigma-Aldrich) according to the manufacturer's instructions. Fluorescence was measured using a FACSCanto II flow cytometer (Becton Dickinson, Franklin Lakes, NJ, USA). The flow cytometry data were analyzed using BD FACS Diva software v6.1.3 (BD Biosciences, San Jose, CA, USA).

### **Colony formation assay**

HCT116 cells were digested with 0.25% trypsin and pipetted into single-cell suspensions, and the cell concentration was adjusted to 200 per dish. After irradiation with variable X-ray doses (0, 2, 4, 6, and 8 Gy) alone or in combination with 20  $\mu$ M andrographolide, the cells were incubated in fresh medium at 37°C in a humidified 5% CO<sub>2</sub> incubator for 48 hours. Cell colony formation was calculated using the following formula: colony formation rate = (number of cell colonies formed/number of cells seeded)  $\times$  100%. The survival fraction was calculated as follows: survival fraction = (colony formation rate of the experimental group/colony formation rate of the control group)  $\times$  100%. The survival fraction of cells was fitted to the cell survival curve according to a linear-quadratic model ( $y = 1 - (1 - \exp(-k \times x))^N$ ) using GraphPad Prism v7.0 (La Jolla, CA, USA).

### **Transwell cell invasion assay**

HCT116 cells were suspended in serum-free medium and adjusted to a density of  $5 \times 10^4$  cells/mL. Then, the cell suspension was added to the upper compartment of the invasion chamber, in which the basement membrane had been coated with 50 mg/L Matrigel (1:8 dilution, Corning, Tokyo, Japan) and 1 mL of culture medium containing 10% FBS. After 48 hours of incubation, the filter membrane was fixed in 95% alcohol for 20 minutes and then stained with hematoxylin for 10 minutes. The cells were then observed and counted under an inverted microscope at  $\times 100$  magnification.

### **Western blotting**

The cell protein was extracted using immunoprecipitation buffer (Auragene, Changsha, China), and samples were centrifuged at 9000 rpm at 4°C for 10 minutes. The protein concentration was determined using a BCA protein assay kit (Auragene). The proteins were separated on 10% SDS-PAGE gels, blotted onto nitrocellulose membranes, and probed with antibodies recognizing PI3K/p85 (1:4000, ab86714, Abcam, Shanghai, China), PI3K/p110 (1:4000, bs-6423R, Bioss, Beijing, China), Akt (1:4000, 21054-1, SAB, Boca Raton, FL, USA), phosphorylated (p)-Akt (Ser473, 1:4000, ab81283, Abcam), mTOR (1:4000, #2972, Cell Signaling Technology, Danvers, MA, USA), p-mTOR (Ser2448) (1:4000, #2971, Cell Signaling Technology), PFK1 (1:4000, sc-377346, Santa Cruz Biotechnology, Santa Cruz, CA, USA), HK2 (1:4000, ab37593, Abcam), or GLUT1 (1:4000, 21829-1-AP, Proteintech, Minneapolis, MN, USA), followed by the appropriate horseradish peroxidase-conjugated secondary antibodies (Auragene). Immunodetection was completed using enhanced chemiluminescence

and a western imprinting system (Auragene). Immunoblotting with anti-GAPDH antibody (1:4000; sc-365062, Santa Cruz Biotechnology) was used as the internal control.

### Statistical analysis

All data were analyzed using GraphPad Prism v7.0. Experimental values are expressed as the mean  $\pm$  SD. The quantitative data were compared using Student's *t*-test. Significance testing of data sets was conducted using analysis of variance (ANOVA). Bonferroni's test and Tukey's

test were used for multiple comparisons. Differences were considered statistically significant at  $P < 0.05$ .

## Results

### Andrographolide inhibited HCT116 cell survival and glycolytic activity in a concentration-dependent manner

The MTT assay was used to measure the survival rate of HCT116 cells treated with different concentrations of andrographolide. The changes of glycolytic activity in

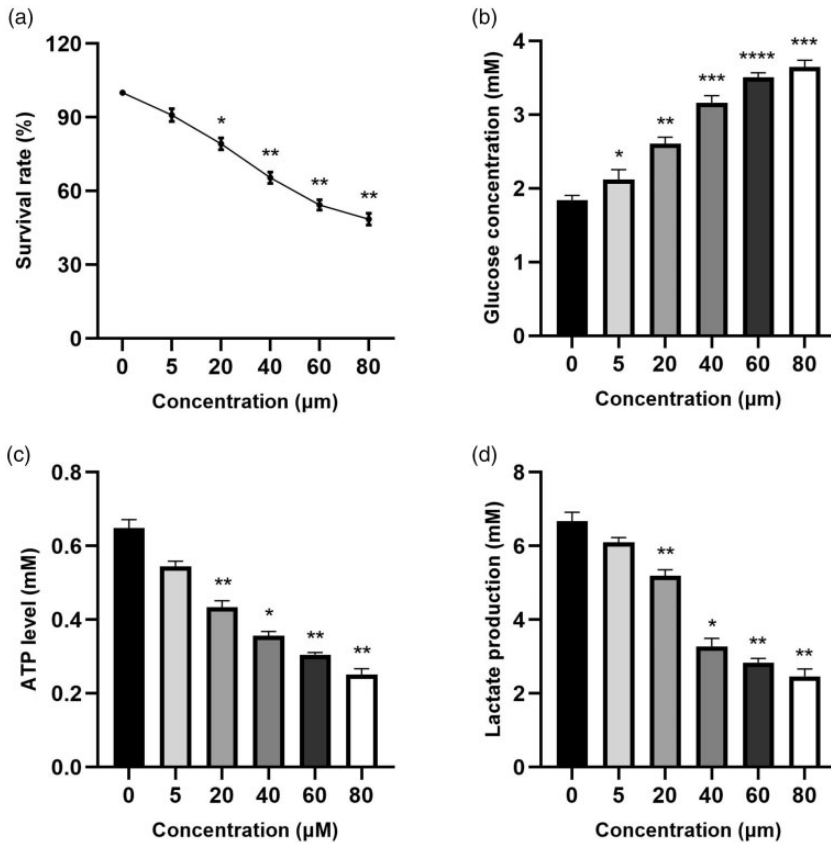


**Figure 1.** HCT116 cell viability and glycolysis levels following treatment with various concentrations of andrographolide. (a) Cell survival rate. (b) Glucose concentration. (c) ATP levels. (d) Lactate production. Data are presented as the mean  $\pm$  SD ( $n = 3$  independent experiments). \* $P < 0.05$ , \*\* $P < 0.01$ , \*\*\* $P < 0.001$ , \*\*\*\* $P < 0.0001$ .

HCT116 cells following treatment were also analyzed. We found that as the andrographolide concentration increased, the survival rate of HCT116 cells decreased, whereas the glucose concentration increased (Figure 1a, b). In addition, the ability of the cells to produce ATP and lactic acid decreased as the andrographolide concentration increased (Figure 1c, d). These results indicated that glucose consumption decreased as the andrographolide concentration increased and that andrographolide inhibited HCT116 cell glycolytic activity in a concentration-dependent manner. The cell survival rate was  $0.792 \pm 0.025$  and the cell proliferation inhibition rate was approximately 20% when the cells were treated with  $20 \mu\text{M}$  andrographolide. Therefore,  $20 \mu\text{M}$  andrographolide was selected for subsequent experiments.

### Andrographolide enhanced the radiosensitivity of HCT116 cells

The effects of andrographolide on the radiosensitivity in HCT116 cells were investigated. The MTT and colony formation assays were performed to measure the survival rate and proliferation of HCT116 cells treated with various doses of radiation (0, 2, 4, 6, and 8 Gy) alone or in combination with  $20 \mu\text{M}$  andrographolide. The MTT assay indicated that the cell survival rate in the combination treatment group was lower than that in the irradiation group (Figure 2). As the radiation dose increased, the colony formation rate decreased, and the decrease was more obvious in the combination treatment group (Figure 3a, b). The colony survival curve illustrated that the colony survival fraction decreased as the radiation dose increased, and the colony survival fraction was significantly lower in the combination treatment group than in the irradiation group ( $P < 0.05$ ; Figure 3c). The mean lethal dose ( $D_0$ ) in the irradiation plus andrographolide

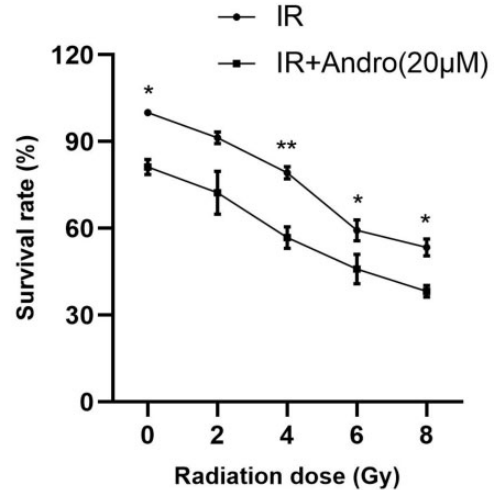


**Figure 2.** The MTT assay was performed to measure the survival of HCT116 cells following treatment with irradiation alone or in combination with  $20 \mu\text{M}$  andrographolide. Data are presented as the mean  $\pm$  SD ( $n = 3$  independent experiments). \* $P < 0.05$ , \*\* $P < 0.01$ .

IR, irradiation; IR+Andro,  $20 \mu\text{M}$  andrographolide plus irradiation.

group was 6.13 Gy, and therefore, 6 Gy was selected as the positive control radiation dose in HCT116 cells.

### Andrographolide regulated HCT116 cell proliferation and glycolytic activity by inhibiting the PI3K-Akt-mTOR signaling pathway

To explore the mechanism by which andrographolide affects proliferation and glycolytic activity in HCT116 cells, we performed western blotting to examine the expression levels of glycolysis-related proteins. The results indicated that the expression of total Akt and total mTOR was similar among the groups. Compared with the findings in the control and IGF-1 groups, PI3K/p110, p-Akt (Ser473), and p-mTOR (Ser2448) expression was significantly downregulated in the andrographolide and LY294002 groups

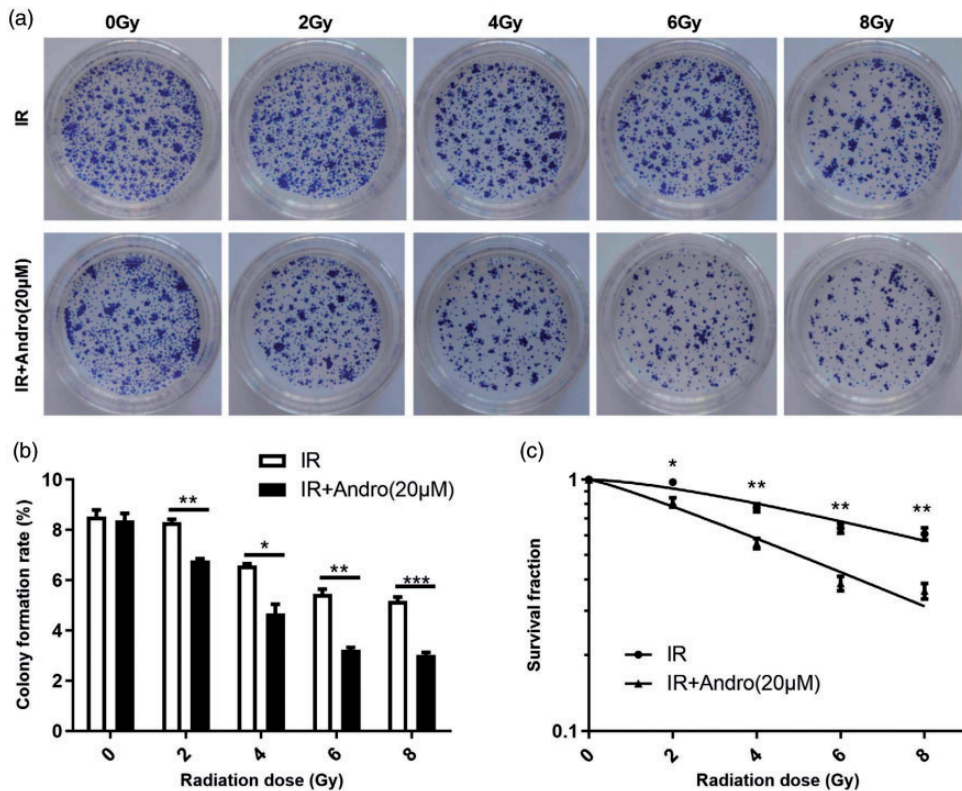


**Figure 3.** Effects of andrographolide on the colony formation and survival of HCT116 cells. (a) Colony formation in the various treatment groups. (b) Cell colony formation rate. (c) The cell survival curve based on the multi-target single-hit mode. Data are presented as the mean  $\pm$  SD ( $n=3$  independent experiments). \* $P < 0.05$ , \*\* $P < 0.01$ , \*\*\* $P < 0.001$ . IR, irradiation; IR+Andro, 20  $\mu$ M andrographolide plus irradiation.

(all  $P < 0.05$ ). In addition, the intracellular glycolysis-related proteins PFK1 and GLUT1 were significantly downregulated (both  $P < 0.05$ ). Another key glycolysis-related enzyme, HK2, was also significantly downregulated in the andrographolide group ( $P < 0.05$ ) but not in the LY294002 group. The results in the andrographolide plus IGF-1 group demonstrated that the effect of andrographolide on PI3K/p110, p-Akt (Ser473), and p-mTOR (Ser2448) expression was suppressed by IGF-1 (Figure 4).

To study whether the changes in PI3K-Akt-mTOR signaling pathway protein

levels were related to glucose metabolism, changes in glycolytic activity in HCT116 cells following andrographolide treatment were measured. As illustrated in Figure 5, glucose metabolism in HCT116 cells was activated following IGF-1 treatment ( $P < 0.05$ ). However, andrographolide suppressed glucose consumption and PFK1 activity and decreased the ability of HCT116 cells to produce lactic acid and ATP (all  $P < 0.05$ ). These results were similar to those in the LY294002 group (all  $P < 0.05$ ). Therefore, andrographolide may affect HCT116 cell glycolytic activity by inhibiting the PI3K-Akt-mTOR signaling

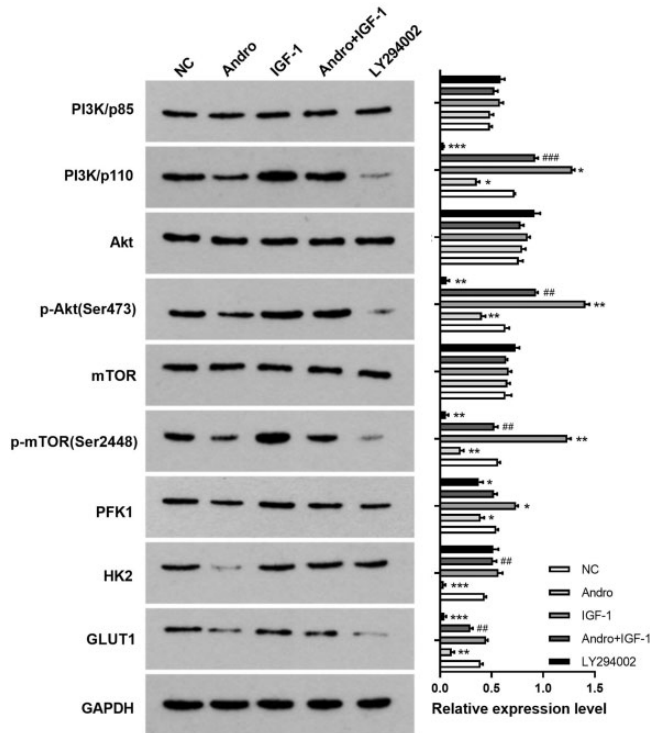


**Figure 4.** Western blotting revealed the expression of glycolysis-related proteins following treatment with andrographolide and a phosphoinositide 3-kinase (PI3K) activator or inhibitor in HCT116 cells. Data are presented as the mean  $\pm$  SD ( $n = 3$  independent experiments). Compared with NC, \* $P < 0.05$ , \*\* $P < 0.01$ , \*\*\* $P < 0.001$ ; Compared with Andro, ### $P < 0.01$ , #### $P < 0.001$ .

NC, Blank control group; Andro, 20  $\mu$ M andrographolide group; IGF-1, PI3K activator group; LY294002, PI3K inhibitor group.

pathway. However, this may not be the only mechanism.

We further conducted experiments to determine whether the effect of andrographolide on HCT116 cell viability was related to the PI3K-Akt-mTOR signaling pathway. The MTT assay results demonstrated that andrographolide and LY294002 decreased the cell survival rate (both  $P < 0.01$ ), whereas IGF-1 promoted cell proliferation (Figure 6). Similarly, in the apoptosis assay, andrographolide and LY294002 promoted apoptosis ( $P < 0.0001$ ), whereas IGF-1 had no significant effect on apoptosis (Figure 7a). In the Transwell assay, IGF-1 significantly enhanced cell

invasion ( $P < 0.0001$ ), whereas andrographolide and LY294002 had the opposite effects (both  $P < 0.001$ , Figure 7b). These results suggest that andrographolide may regulate HCT116 cell survival by inhibiting the PI3K-Akt-mTOR signaling pathway.

#### *Andrographolide enhanced the radiosensitivity of HCT116 cells by regulating the PI3K-Akt-mTOR signaling pathway*

To determine the molecular mechanisms of the effects of andrographolide on HCT116 cell radiosensitivity, we measured the expression levels of glycolysis-related

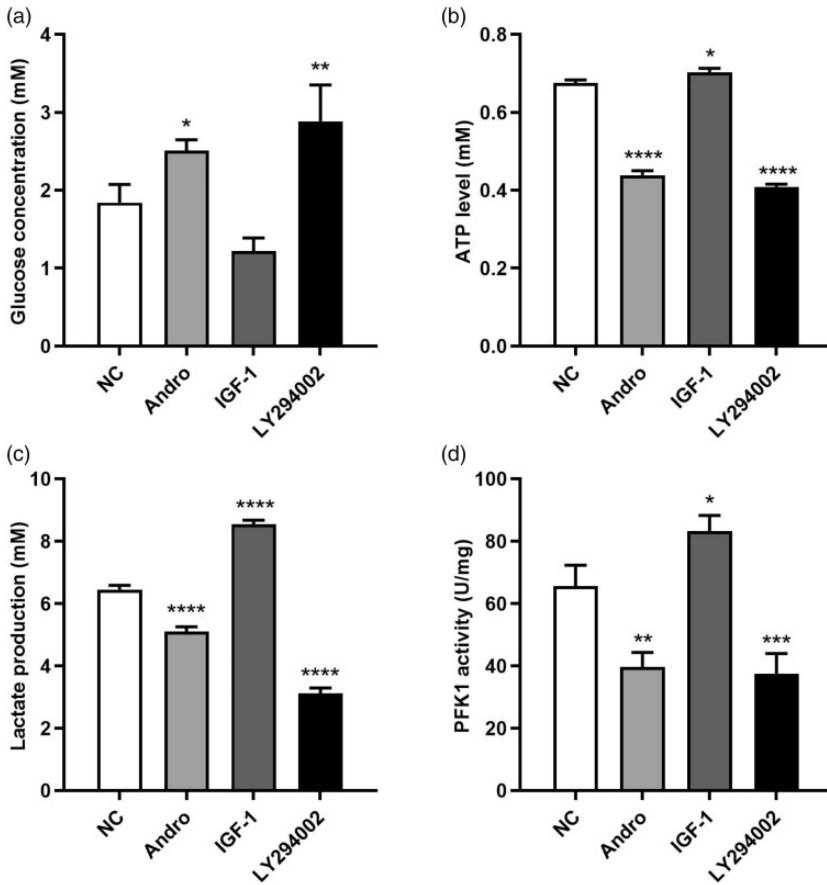


**Figure 5.** Changes in glucose concentrations (a), ATP levels (b), lactate production (c), and phospho-fructokinase-1 (PFK1) activity (d) in HCT116 cells treated with andrographolide and a phosphoinositide 3-kinase (PI3K) activator or inhibitor. Data are presented as the mean  $\pm$  SD ( $n = 3$  independent experiments). \* $P < 0.05$ , \*\* $P < 0.01$ , \*\*\* $P < 0.001$ , \*\*\*\* $P < 0.0001$ .

NC, Blank control group; Andro, 20  $\mu$ M andrographolide group; IGF-1, PI3K activator group; LY294002, PI3K inhibitor group.

proteins in HCT116 cells treated with 6 Gy of irradiation alone or in combination with andrographolide. Via western blot analysis, we found that PI3K-Akt-mTOR signaling pathway-related proteins, the key glycolysis enzymes PFK1 and HK2, and GLUT1 were all downregulated after treatment with 6 Gy of irradiation (all  $P < 0.05$ ). In addition, PI3K/p110, p-Akt (Ser473), p-mTOR (Ser2448), PFK1, and HK2 expression was lower in the

andrographolide plus irradiation and LY294002 plus irradiation groups than in the irradiation group (Figure 8). The glycolysis assay revealed that irradiation suppressed glucose consumption and PFK1 activity and decreased the ability of HCT116 cells to produce lactic acid and ATP (all  $P < 0.01$ , Figure 9). Moreover, irradiation plus andrographolide or LY294002 further decreased PFK1 activity and the ability of HCT116 cells to produce

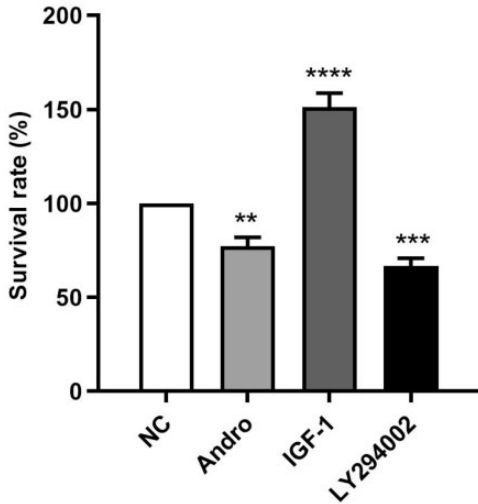


**Figure 6.** Changes in the viability of HCT116 cells treated with andrographolide and a phosphoinositide 3-kinase (PI3K) activator or inhibitor. Data are presented as the mean  $\pm$  SD ( $n = 3$  independent experiments). \*\* $P < 0.01$ , \*\*\* $P < 0.001$ , \*\*\*\* $P < 0.0001$ . NC, Blank control group; Andro, 20  $\mu$ M andrographolide group; IGF-1, PI3K activator group; LY294002, PI3K inhibitor group.

lactic acid and ATP compared with the effects of radiation alone (all  $P < 0.001$ ).

Next, the MTT assay was used to measure the survival rate of HCT116 cells exposed to radiation alone or in combination with andrographolide. The survival rates in the andrographolide plus irradiation and LY294002 plus irradiation groups were significantly lower than that in the irradiation group (both  $P < 0.05$ ). There was no significant difference between the first two groups (Figure 10). In the apoptosis assay, the apoptosis rate of the cells increased after treatment with 6 Gy of radiation ( $P < 0.0001$ , Figure 11a). Compared with the findings in cells exposed to irradiation, the apoptosis rate was significantly higher in the andrographolide plus irradiation group, and the same result was obtained in the LY294002 plus irradiation group (both  $P < 0.0001$ ). We further

performed Transwell and colony formation assays. Cell invasion and colony formation rates were significantly lower in the andrographolide plus irradiation and LY294002 plus irradiation groups than in the irradiation group (both  $P < 0.001$ ; Figure 11b, c), indicating that andrographolide might enhance the radiosensitivity of HCT116 cells by regulating the PI3K-Akt-mTOR signaling pathway.

## Discussion

Prior studies revealed that many genes in CRC cells, such as retinoblastoma-binding protein 6, CC motif chemokine receptor 6, and miR-622, are closely related to radiosensitivity.<sup>17–19</sup> Inhibition of the expression of these genes can enhance the radiosensitivity of CRC cells. However, these methods cannot be applied to patients clinically because of the lack of technology. Although chemotherapeutic drugs induce toxicity, they are commonly used for radiosensitization.<sup>20</sup> Plant extracts, especially Chinese herbals, cause less toxicity than synthetic drugs. In recent years, Chinese herbal extracts have been investigated extensively in tumor radiosensitization experiments. Many studies illustrated that some Chinese herbal monomers, such as curcumin, icariin, and genistein derivatives, enhance radiosensitivity in HT29 and HCT116 cells.<sup>21–23</sup>

Andrographolide is an active ingredient extracted from the traditional Chinese medicine *A. paniculata* that has been revealed to exert prophylactic therapeutic effects and increase chemosensitivity in CRC cells. Andrographolide can inhibit the growth of colon cancer cells by selectively increasing the levels of reactive oxygen species, inhibiting the Akt/mTOR signaling pathway, interfering with the cell cycle, and inducing apoptosis.<sup>24</sup> In addition, andrographolide increases the radiosensitivity of oral squamous carcinoma, esophageal cancer, and

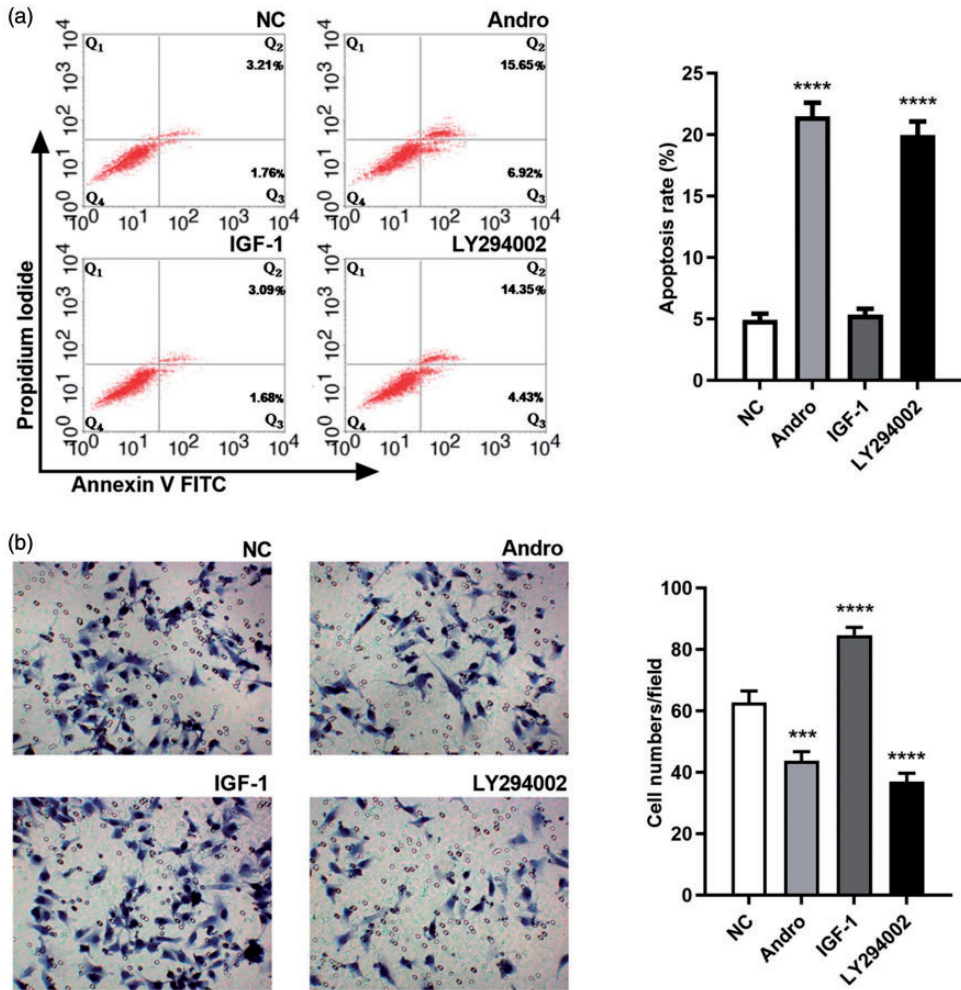


**Figure 7.** Effects of various treatments on invasion and apoptosis in HCT116 cells. (a) Apoptosis detected by flow cytometry. (b) Cell invasive ability detected using the Transwell assay. Data are presented as the mean  $\pm$  SD ( $n = 3$  independent experiments). \*\*\* $P < 0.001$ , \*\*\*\* $P < 0.0001$ . NC, Blank control group; Andro, 20  $\mu$ M andrographolide group; IGF-1, PI3K activator group; LY294002, PI3K inhibitor group.

ovarian cancer cells.<sup>25–27</sup> To our knowledge, the effects of andrographolide on radiosensitivity in CRC cells and the possible mechanisms of action had not been reported.

In our study, we found that the cytotoxic effect of andrographolide in HCT116 cells was concentration-dependent. At an andrographolide concentration of 20  $\mu$ M,

the cell survival rate was  $0.792 \pm 0.025$ , and the cell proliferation inhibition rate was approximately 20%. Therefore, this concentration was used in combination with different doses of radiation to explore the effect on radiosensitivity in HCT116 cells. Both the MTT and colony formation assays demonstrated that andrographolide enhanced the radiosensitivity of HCT116

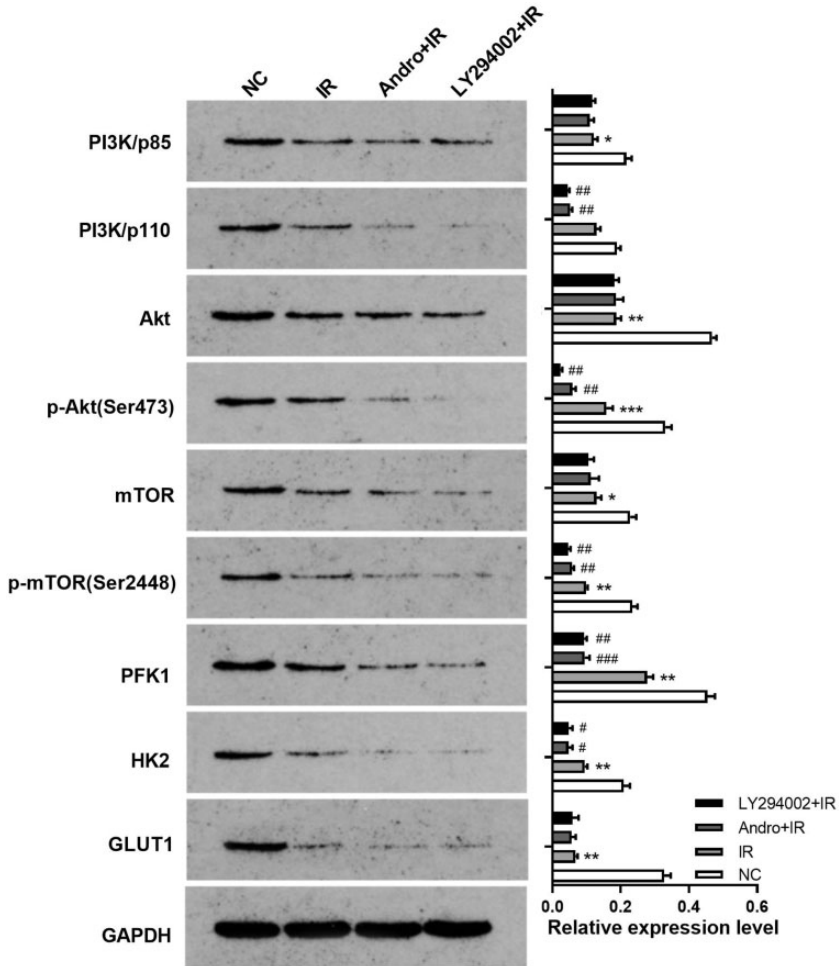


**Figure 8.** Western blotting assay revealed the expression of glycolysis-related proteins following treatment with irradiation alone or in combination with 20  $\mu$ M andrographolide in HCT116 cells. Data are presented as the mean  $\pm$  SD (n = 3 independent experiments). Compared with NC, \* $P$  < 0.05, \*\* $P$  < 0.01, \*\*\* $P$  < 0.001; Compared with IR group, # $P$  < 0.05, ## $P$  < 0.01, ### $P$  < 0.001. NC, Blank control group; IR, irradiation group; Andro+IR, andrographolide plus irradiation group; LY294002+IR, PI3K inhibitor plus irradiation group.

cells. The sensitive enhancement ratio D0 of 20  $\mu$ M andrographolide plus irradiation in HCT116 cells was 1.496.

Metabolic reprogramming, especially cellular glucose metabolism, is a prominent feature of malignant tumors.<sup>26</sup> Even in the presence of adequate oxygen, most malignant tumors obtain needed energy and

nutrition through glycolysis, which produces lactic acid. Lactic acid provides an acidic microenvironment for tumor cells and promotes cell metastasis and invasion.<sup>27</sup> In our study, the changes of glycolytic activity in HCT116 cells were monitored following treatment. We found that glucose consumption, ATP

production, lactic acid production, and PFK1 activity decreased gradually as the andrographolide concentration increased. Andrographolide inhibited glycolytic activity concentration-dependently in HCT116 cells.

Molecular biological studies have revealed that many key mutations and changes in signaling pathways can alter the metabolism of tumor cells to allow them to adapt to rapid cell growth.<sup>28</sup> The PI3K pathway plays an important role in

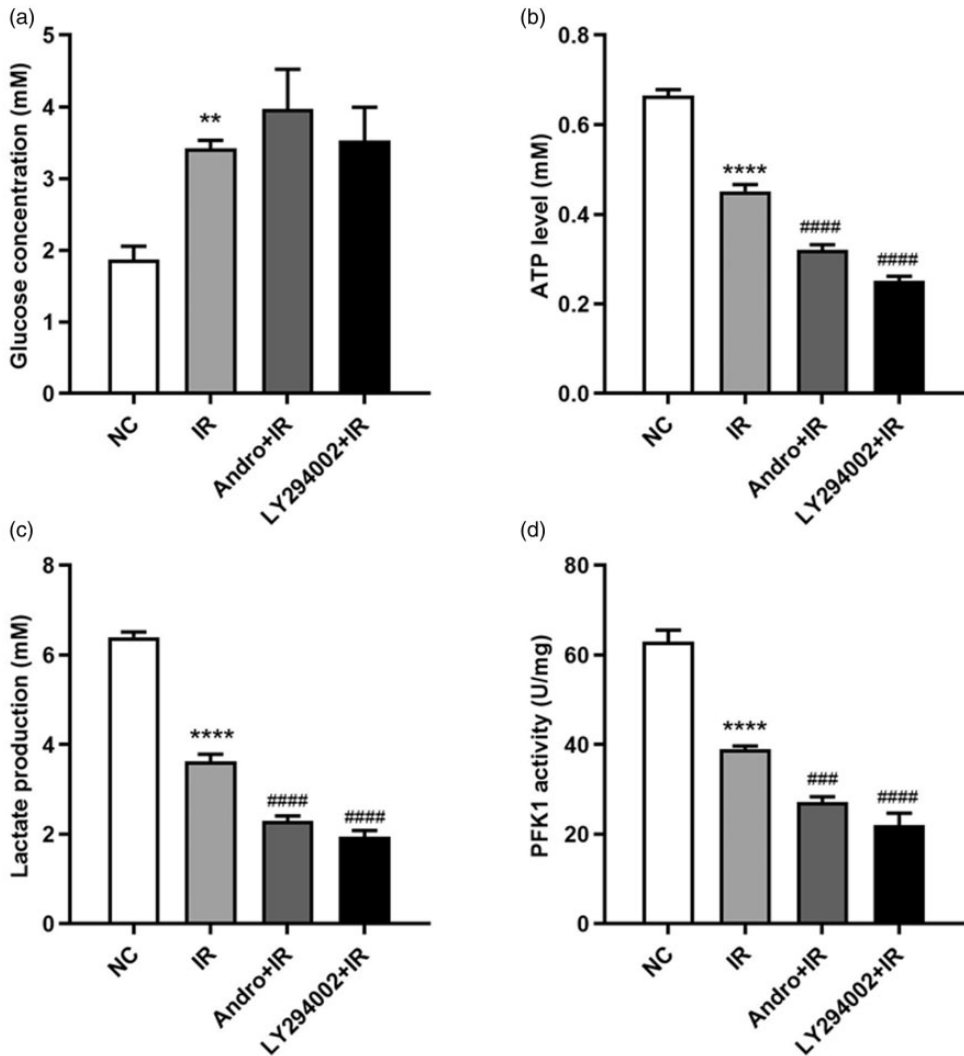


**Figure 9.** Changes in glucose concentrations (a), ATP levels (b), lactate production (c), and PFK1 activity (d) in HCT116 cells treated with irradiation, irradiation plus 20  $\mu$ M andrographolide, and irradiation plus a phosphoinositide 3-kinase (PI3K) inhibitor. The data are presented as the mean  $\pm$  SD ( $n = 3$  independent experiments). Compared with NC, \*\* $P < 0.01$ , \*\*\* $P < 0.0001$ ; Compared with IR group, #### $P < 0.001$ , ##### $P < 0.0001$ .

NC, Blank control group; IR, irradiation group; Andro+IR, andrographolide plus irradiation group; LY294002+IR, PI3K inhibitor plus irradiation group.

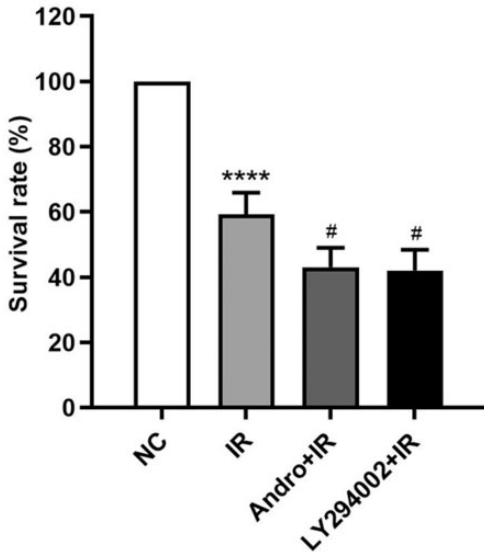


**Figure 10.** Changes in the viability of HCT116 cells treated with irradiation, irradiation plus 20  $\mu$ M andrographolide, and irradiation plus a phosphoinositide 3-kinase (PI3K) inhibitor. Data are presented as the mean  $\pm$  SD (n = 3 independent experiments). Compared with NC, \*\*\*\* $p < 0.0001$ ; Compared with IR group, # $p < 0.05$ . NC, Blank control group; IR, irradiation group; Andro+IR, andrographolide plus irradiation group; LY294002+IR, PI3K inhibitor plus irradiation group.

tumor cell metabolism. Akt is a potent regulator of aerobic glycolysis downstream of PI3K. In addition to regulating glycolytic enzymes directly, PI3K can activate Akt and stimulate glycolysis by activating mTOR. The radioresistance of tumor cells is closely related to cell glycolysis. For example, the overexpression of HK2, a key enzyme of glycolysis, is positively correlated with radioresistance in various tumors including laryngeal cancer, liver cancer, glioma, and prostate cancer.<sup>13</sup> Studies have demonstrated that andrographolide can suppress glycolysis, reduce cell proliferation by inhibiting the PI3K-Akt pathway, and suppress chemotactic migration by inhibiting ERK1/2 and Akt phosphorylation.<sup>29-31</sup> It also has been reported

that the radiosensitivity of tumor cells can be regulated by inhibiting the PI3K-Akt-mTOR or EGFR-PI3K-Akt-mTOR signaling pathway directly.<sup>32,33</sup>

Our previous study demonstrated that the expression of the glycolysis-related proteins GLUT1, lactate dehydrogenase isoform A, and HK2 was downregulated and the radiosensitivity of hepatoma cells was enhanced *in vitro* and *in vivo* after silencing the Girdin gene, which lies upstream of the PI3K-Akt-mTOR signaling pathway.<sup>16</sup> In our study, we confirmed that andrographolide inhibited phosphorylation in the PI3K-Akt-mTOR signaling pathway and downregulated the expression of PFK1, HK2, and GLUT1 in glycolysis. IGF-1, a PI3K activator, can activate the PI3K/Akt signaling pathway and increase Akt phosphorylation.<sup>34</sup> In our study, we further found that IGF-1 could reverse the downregulation of PI3K/p110, p-Akt (Ser473), and p-mTOR (Ser2448) in HCT116 cells induced by andrographolide. Moreover, LY294002 is a widely used PI3K inhibitor. Our results indicated that andrographolide inhibited the survival, invasion, and proliferation of HCT116 cells and increased the apoptosis rate, which were similar to the effects of LY294002. Based on these results, we speculated that andrographolide enhanced radiosensitivity by downregulating glycolysis or inhibiting the PI3K-Akt-mTOR signaling pathway in HCT116 cells. However, the changes in expression were not identical between the andrographolide and LY294002 groups, indicating that inhibition of the PI3K-Akt-mTOR signaling pathway is not the only mechanism by which andrographolide increases the radiosensitivity of HCT116 cells.

Traditional Chinese herbal monomers have multiple targets, and the potential mechanisms of action require further exploration. One limitation of this study was the lack of an *in vivo* animal model. In addition, further experiments are needed to verify

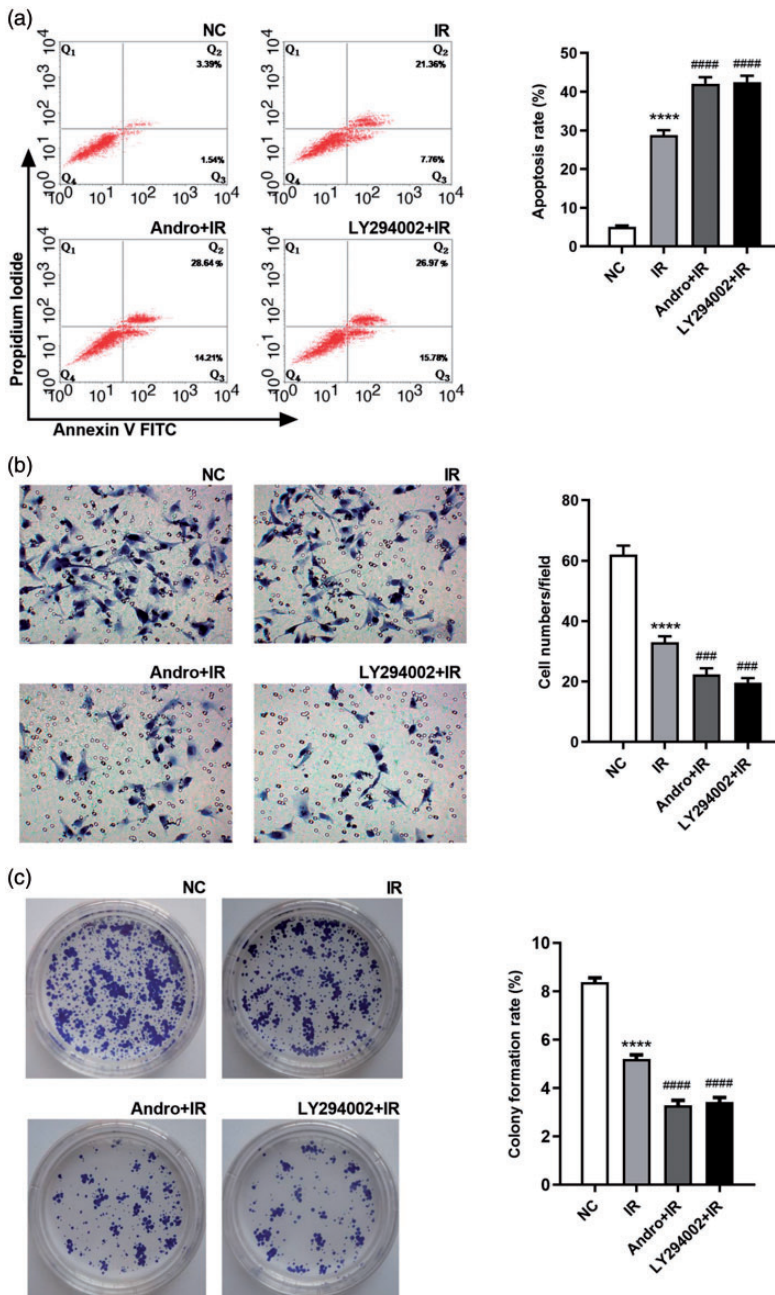


**Figure 11.** Apoptosis, invasion, and colony formation rates of HCT116 cells treated with irradiation, irradiation plus 20  $\mu$ M andrographolide, and irradiation plus a phosphoinositide 3-kinase (PI3K) inhibitor. (a) Cell apoptosis detected by flow cytometry. (b) Cell invasive ability detected using the Transwell assay. (c) Colony formation. Data are presented as the mean  $\pm$  SD (n = 3 independent experiments). Compared with NC, \*\*\*P < 0.0001; Compared with IR group, ####P < 0.001, #####P < 0.0001. NC, Blank control group; IR, irradiation group; Andro+IR, andrographolide plus irradiation group; LY294002+IR, PI3K inhibitor plus irradiation group.

whether andrographolide can enhance radiosensitivity in other CRC cells, such as HT29 cells.

## Conclusions

Our study demonstrated that andrographolide enhanced the radiosensitivity of HCT116 cells and that this effect may be related to the regulation of PI3K-Akt-mTOR signaling and inhibition of glycolysis.

## Declaration of conflicting interest

The authors declare that there is no conflict of interest.

## Funding

This research received no specific grant from any funding agency in the public, commercial, or not-for-profit sectors.

## ORCID iDs

Ruifang Tian  <https://orcid.org/0000-0002-3333-1944>

Chenghui Huang  <https://orcid.org/0000-0003-2110-2172>

## References

1. Siegel RL, Miller KD and Jemal A. Cancer statistics, 2019. *CA Cancer J Clin* 2019; 69: 7–34.
2. Lorimer PD, Motz BM, Kirks RC, et al. Pathologic Complete Response Rates After Neoadjuvant Treatment in Rectal Cancer: an Analysis of the National Cancer Database. *Ann Surg Oncol* 2017; 24: 2095–2103.
3. Lee AW, Ng WT, Hung WM, et al. Major late toxicities after conformal radiotherapy for nasopharyngeal carcinoma-patient- and treatment-related risk factors. *Int J Radiat Oncol Biol Phys* 2009; 73: 1121–1128.
4. Kandanur SGS, Tamang N, Golakoti NR, et al. Andrographolide: a natural product template for the generation of structurally and biologically diverse diterpenes. *Eur J Med Chem* 2019; 176: 513–533.
5. Soo HL, Quah SY, Sulaiman I, et al. Advances and challenges in developing andrographolide and its analogues as cancer therapeutic agents. *Drug Discov Today* 2019; 24: 1890–1898.
6. Yang PY, Hsieh PL, Wang TH, et al. Andrographolide impedes cancer stemness and enhances radio-sensitivity in oral carcinomas via miR-218 activation. *Oncotarget* 2017; 8: 4196–4207.
7. Wang ZM, Kang YH, Yang X, et al. Andrographolide radiosensitizes human esophageal cancer cell line ECA109 to radiation in vitro. *Dis Esophagus* 2016; 29: 54–61.
8. Guo W, Sun Y, Liu W, et al. Small molecule-driven mitophagy-mediated NLRP3 inflammasome inhibition is responsible for the prevention of colitis-associated cancer. *Autophagy* 2014; 10: 972–985.
9. Courtney R, Ngo DC, Malik N, et al. Cancer metabolism and the Warburg effect: the role of HIF-1 and PI3K. *Mol Biol Rep* 2015; 42: 841–851.
10. Chaurasia A, Kharya MD, Sharma B, et al. Glucose metabolism and diabetogenic gene expression analysis of chloroform fraction of *Andrographis paniculata* (Nees) whole herb in diabetic albino mice. *J Complement Integr Med* 2012; 9: Article 21.
11. Subramanian R, Asmawi MZ and Sadikun A. In vitro alpha-glucosidase and alpha-amylase enzyme inhibitory effects of *Andrographis paniculata* extract and andrographolide. *Acta Biochim Pol* 2008; 55: 391–398.
12. Lenzen S. A fresh view of glycolysis and glucokinase regulation: history and current status. *J Biol Chem* 2014; 289: 12189–12194.
13. Zhong JT and Zhou SH. Warburg effect, hexokinase-II, and radioresistance of laryngeal carcinoma. *Oncotarget* 2017; 8: 14133–14146.
14. Meng MB, Wang HH, Guo WH, et al. Targeting pyruvate kinase M2 contributes to radiosensitivity of non-small cell lung cancer cells in vitro and in vivo. *Cancer Lett* 2015; 356: 985–993.

15. Zhao Y, Shen L, Chen X, et al. High expression of PKM2 as a poor prognosis indicator is associated with radiation resistance in cervical cancer. *Histol Histopathol* 2015; 30: 1313–1320.
16. Yu L, Sun Y, Li J, et al. Silencing the Girdin gene enhances radio-sensitivity of hepatocellular carcinoma via suppression of glycolytic metabolism. *J Exp Clin Cancer Res* 2017; 36: 110.
17. Xiao C, Wang Y, Zheng M, et al. RBBP6 increases radioresistance and serves as a therapeutic target for preoperative radiotherapy in colorectal cancer. *Cancer Sci* 2018; 109: 1075–1087.
18. Chang H, Wei JW, Tao YL, et al. CCR6 Is a Predicting Biomarker of Radiosensitivity and Potential Target of Radiosensitization in Rectal Cancer. *Cancer Res Treat* 2018; 50: 1203–1213.
19. Ma W, Yu J, Qi X, et al. Radiation-induced microRNA-622 causes radioresistance in colorectal cancer cells by down-regulating Rb. *Oncotarget* 2015; 6: 15984–15994.
20. Matsuoka K, Kobunai T, Nukatsuka M, et al. Improved chemoradiation treatment using trifluridine in human colorectal cancer cells in vitro. *Biochem Biophys Res Commun* 2017; 494: 249–255.
21. Yang G, Qiu J, Wang D, et al. Traditional Chinese Medicine Curcumin Sensitizes Human Colon Cancer to Radiation by Altering the Expression of DNA Repair-related Genes. *Anticancer Res* 2018; 38: 131–136.
22. Zhang Y, Wei Y, Zhu Z, et al. Icarin enhances radiosensitivity of colorectal cancer cells by suppressing NF-kappaB activity. *Cell Biochem Biophys* 2014; 69: 303–310.
23. Gruca A, Krawczyk Z, Szeja W, et al. Synthetic genistein glycosides inhibiting EGFR phosphorylation enhance the effect of radiation in HCT 116 colon cancer cells. *Molecules* 2014; 19: 18558–18573.
24. Banerjee A, Banerjee V, Czinn S, et al. Increased reactive oxygen species levels cause ER stress and cytotoxicity in andrographolide treated colon cancer cells. *Oncotarget* 2017; 8: 26142–26153.
25. Zhang C and Qiu X. Andrographolide radiosensitizes human ovarian cancer SKOV3 xenografts due to an enhanced apoptosis and autophagy. *Tumour Biol* 2015; 36: 8359–8365.
26. Pavlova NN and Thompson CB. The Emerging Hallmarks of Cancer Metabolism. *Cell Metab* 2016; 23: 27–47.
27. Baig MH, Adil M, Khan R, et al. Enzyme targeting strategies for prevention and treatment of cancer: implications for cancer therapy. *Semin Cancer Biol* 2019; 56: 1–11.
28. Cairns RA, Harris IS and Mak TW. Regulation of cancer cell metabolism. *Nat Rev Cancer* 2011; 11: 85–95.
29. Yao H, Wu Z, Xu Y, et al. Andrographolide attenuates imbalance of gastric vascular homeostasis induced by ethanol through glycolysis pathway. *Sci Rep* 2019; 9: 4968.
30. Kayastha F, Madhu H, Vasavada A, et al. Andrographolide reduces proliferation and migration of lens epithelial cells by modulating PI3K/Akt pathway. *Exp Eye Res* 2014; 128: 23–26.
31. Tsai HR, Yang LM, Tsai WJ, et al. Andrographolide acts through inhibition of ERK1/2 and Akt phosphorylation to suppress chemotactic migration. *Eur J Pharmacol* 2004; 498: 45–52.
32. Horn D, Hess J, Freier K, et al. Targeting EGFR-PI3K-AKT-mTOR signaling enhances radiosensitivity in head and neck squamous cell carcinoma. *Expert Opin Ther Targets* 2015; 19: 795–805.
33. Chang L, Graham PH, Ni J, et al. Targeting PI3K/Akt/mTOR signaling pathway in the treatment of prostate cancer radioresistance. *Crit Rev Oncol Hematol* 2015; 96: 507–517.
34. Rommel C, Bodine SC, Clarke BA, et al. Mediation of IGF-1-induced skeletal myotube hypertrophy by PI(3)K/Akt/mTOR and PI(3)K/Akt/GSK3 pathways. *Nat Cell Biol* 2001; 3: 1009–1013.